

SCIENTIFIC REPORTS

OPEN

Nanowire CdS-CdTe Solar Cells with Molybdenum Oxide as Contact

Hongmei Dang & Vijay P. Singh

Received: 08 February 2015

Accepted: 04 September 2015

Published: 06 October 2015

Using a 10 nm thick molybdenum oxide (MoO_{3-x}) layer as a transparent and low barrier contact to p-CdTe, we demonstrate nanowire CdS-CdTe solar cells with a power conversion efficiency of 11% under front side illumination. Annealing the as-deposited MoO_3 film in N_2 resulted in a reduction of the cell's series resistance, from $9.97 \Omega/\text{cm}^2$ to $7.69 \Omega/\text{cm}^2$, and increase in efficiency from 9.9% to 11%. Under illumination from the back, the $\text{MoO}_{3-x}/\text{Au}$ side, the nanowire solar cells yielded J_{sc} of $21 \text{ mA}/\text{cm}^2$ and efficiency of 8.67%. Our results demonstrate use of a thin layer transition metal oxide as a potential way for a transparent back contact to nanowire CdS-CdTe solar cells. This work has implications toward enabling a novel superstrate structure nanowire CdS-CdTe solar cell on Al foil substrate by a low cost roll-to roll fabrication process.

CdTe¹, Cu(In,Ga)Se₂², Cu₂ZnSn(S,Se)₄³, silicon⁴, and perovskites⁵ are among the leading photovoltaic technologies being developed to generate low-cost solar electricity. In particular, CdTe photovoltaics have energy return investment exceeding that of traditional fossil fuels and provide the shortest energy payback time among all photovoltaic technologies for terrestrial applications⁶. In addition, CdTe photovoltaics have superior tolerance to high energy irradiation and are more suitable for space applications⁷.

Development of a transparent and stable contact to the CdTe absorber layer has remained challenging and is of great interest because it can further advance the technology where CdTe solar cells are fabricated on flexible foils of metals in a superstrate device structure. The metal foil-based CdTe solar cells can be implemented by a high-throughput roll-to-roll manufacturing process, resulting in significant cost reduction, high material utilization and fabrication scalability⁷. Traditionally, CdTe solar cells on metal foils are configured with an inverted substrate structure^{6,7}. However, CdTe solar cells using the substrate structure yield lower efficiency values than their superstrate counterparts⁷. The substrate structure imposes many restriction on process optimization, for example, the rather difficult etching process on the CdTe layer prior to contact formation, diffusion of impurities to the contact of CdTe, and CdCl_2 treatment effect on CdS and CdTe layer^{6,7}. Hence, formation of superstrate structured CdTe solar cells on metal foils is one of the most promising options for low cost and high efficiency photovoltaic technologies.

Recently, we have developed nanowire CdS-CdTe solar cells to address light absorption loss and interface recombination issues⁸⁻¹¹, where CdS nanowires embedded in a transparent anodic aluminum oxide (AAO) membrane replace planar CdS as the window layer and CdTe is deposited on the top of the CdS nanowires (Fig. 1a)¹². Such nanowire CdS-CdTe solar cells reduced light absorption loss in the low wavelength region by confinement effects of nanostructures⁸⁻¹¹, and exhibited a nearly ideal spectral response of quantum efficiency from 335 nm to 850 nm, which is the cut-off wavelength corresponding to the bandgap of the CdTe absorber. Next, it was thought that the development of a transparent back contact for CdTe film would lead to a nanowire CdS-CdTe solar cells that would allow the shining of sunlight through the back contact and thus realize the superstrate configuration (Fig. 1b). Because AAO is formed by anodizing aluminum, the nanowire CdS-CdTe solar cells can be grown on aluminum foil; this makes the roll-to-roll manufacturing process feasible and greatly reduces the complexity of fabrication (Fig. 1c).

Department of Electrical and Computer Engineering, and Center for Nanoscale Science and Engineering (CeNSE), University of Kentucky, Lexington, KY, 40506-0046, USA. Correspondence and requests for materials should be addressed to V.P.S. (email: vsingh@uky.edu)

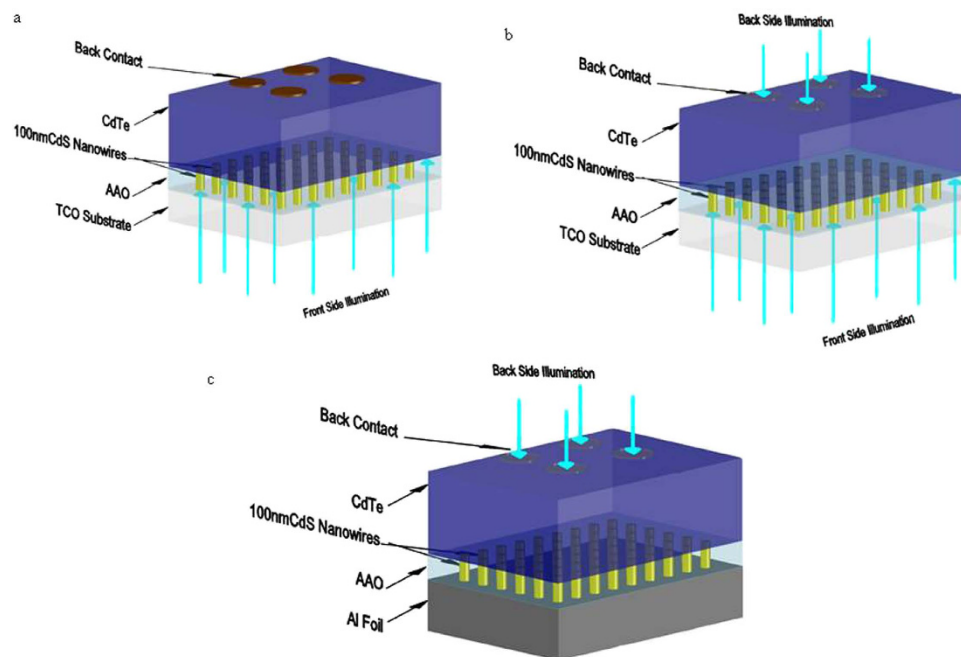


Figure 1. (a) Schematic of a CdS nanowire window layer-CdTe absorber solar cell on TCO substrate illuminated from front side. (b) Schematic of a CdS nanowire window layer-CdTe absorber solar cell on TCO substrate with almost transparent back contacts which can be illuminated from front and back side. (c) Schematic of a CdS nanowire window layer-CdTe absorber solar cell on Al foil with almost transparent back contacts which can be illuminated from back side.

Several types of metal oxides have been investigated as buffer layer to low barrier back contacts¹³. In this work, molybdenum oxide (MoO_3) is studied as a transparent back contact to the CdTe absorber layer, due to its high transparency (higher than 80%) in the visible and near IR range and its behavior is like that of a high work function metal^{14–16}. In addition, its electrical and optical properties can be tuned by controlling the oxygen stoichiometry during processing. Several groups have applied MoO_3/Ni and MoO_3/Au back contacts into CdS/CdTe solar cells and reported 12.2–14.1% values for power conversion efficiency^{17–19}. Here, we investigate the effects of a thin MoO_3/Au layer as the transparent back contact on the nanowire solar cells through front and back side illuminations. We further investigate possibility of reducing resistance of MoO_3 back contacts due to its insulation property by post-processing annealing. In the following sections, the effects of the MoO_3/Au back contact layer on the structural and device properties of the nanowire CdS-CdTe solar cells are demonstrated and their loss mechanism and further improvement are discussed.

Experimental procedures

The nanowire CdS/CdTe solar cells are prepared by our previously established methods¹². The solar cells were fabricated on ITO coated soda-lime glass substrates with sheet resistance of 23–28 Ω/square . The fabrication processes include formation of AAO membrane by anodizing aluminum film, electro-deposition of CdS nanowires with 100 nm height, close-space sublimation of CdTe to a thickness of 10 μm , and CdCl_2 treatments at 400 °C. Without NP etch, MoO_3 thin films with a thickness of 10 nm were thermally evaporated on clean CdTe surfaces from stoichiometric MoO_3 powder (Alfa Aesar, 99.9%), where the pressure was less than 1×10^{-5} Torr and the deposition rate was maintained as 0.5 $\text{\AA}/\text{s}$. Samples were masked and then annealed at 200 °C in N_2 for 10 mins. In the last step, 15 nm Au was deposited by sputtering process. For a comparative study, after thermal evaporation of molybdenum oxide, samples were directly coated with 15 nm of Au without the intervening annealing step. After depositing Au layer, all of the samples were annealed at 200 °C in Argon for 10 mins. Structures of CdS nanowires embedded in AAO templates were characterized via scanning electron microscopy (S-900-SEM). Current–voltage ($I-V$) was measured by a solar simulator set at 100 mW/cm^2 , calibrated by a power meter.

Results and Discussion

Materials Characterization. CdS nanowires are characterized by scanning electron microscopy (SEM). Figure 2a shows free standing CdS nanowires where AAO membrane has been completely removed by a highly selective NaOH solution. Figure 2b shows cross-sectional view of CdS nanowires. As seen in Fig. 2b, CdS nanowires are embedded in AAO nanopores; often, a few nanopores are seen to be missing their CdS nanowires; these, very likely, were knocked off from the AAO nanopores during the sample

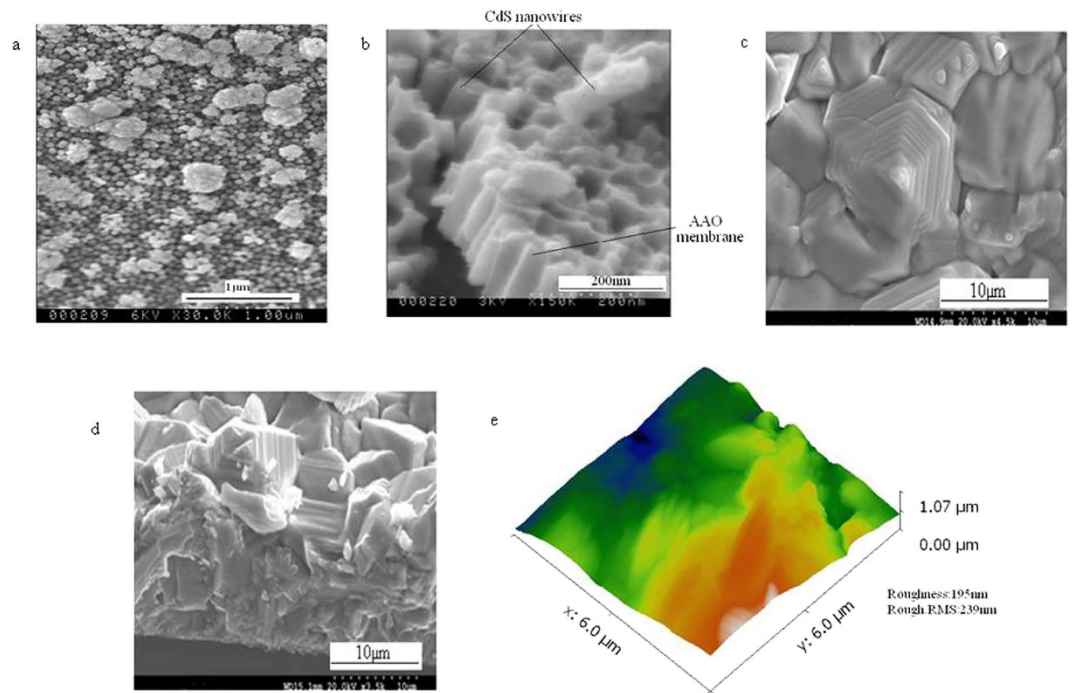


Figure 2. (a) Top view SEM image of free-standing CdS nanowires, (b) Cross-sectional view SEM images of CdS nanowires embedded in AAO membrane, (c) Top view SEM image of CdTe film, (d) cross-section view of CdTe film. (e) The AFM image of the top view of CdTe.

preparation steps for the SEM viewing. The sample preparation for cross section requires scoring the film hard so that from the shock, a fracture exposing the cross section is achieved.

On the other hand, in the SEM sample preparation for the top view (Fig. 2a), no such fracturing shock is required. In the top views of our films, all the AAO pores are in fact filled by the CdS nanowires.

Overall, CdS nanowires form uniform and dense arrays; values of the average length of nanowires, the average diameter and the average distance between the centers of neighboring nanowires are 100 nm, 60 nm and 106 nm respectively. Based on the CdS nanowires features, porosity is approximately 32% and area density of CdS nanowires is calculated as approximately 1.14×10^{10} nanowires/cm². This high density CdS nanowire array was grown perpendicular to the glass-ITO substrate, but can also be directly grown on aluminum foil and other flexible substrates. These embedded CdS nanowires function as the window layer and are configured into the CdS nanowire window layer-CdTe absorber layer solar cells.

Figure 2c,d show the surface morphologies of CdTe film and cross-section view of CdTe film. It is obvious that CdTe film have a compact morphology, consisting of crystallites with grain size between average 6 μm to 7 μm. Observed from cross section SEM images of the CdTe film, it is estimated that thickness of CdTe is the 10 μm–15 μm. Figure 2e shows the AFM image of the top view of CdTe. For 6*6 μm² CdTe area, the roughness and roughness rms values are 195 nm and 239 nm.

Quantum Efficiency of the Nanowire CdS-CdTe Solar Cells. Quantum efficiency characterization is especially interesting in exploring how the CdS nanowires embedded in the AAO membrane as the window layer effectively improve light transmission and how the nanowire CdS-CdTe solar cells effectively absorb light and generate and collect carriers by confinement effects of nanostructures^{8–11}. The normalized external quantum efficiency (EQE) of a typical nanowire solar cell is shown in Fig. 3. These nanowire solar cells were fabricated on intrinsic SnO₂/commercially available ITO-soda lime glass substrate with low transparency and high resistivity.

As shown in Fig. 3, the nanowire CdS-CdTe solar cells exhibit relatively strong quantum efficiency response from 345 nm to 845 nm, which is the bandgap edge of CdTe absorber. Such EQE response indicates that a very wide spectral range of incident photons is almost completely absorbed and photo-generated carriers are effectively collected. It is clear that CdS nanowires embedded in transparent AAO membrane effectively enhance transmission of the window layer. As a result, the wide spectrum of sunlight above 345 nm can be directed into the CdTe absorber where photons are absorbed and converted into charge carriers. Thus by using the embedded CdS nanowires as the window layer, abilities of carrier generation and collection in the CdS-CdTe solar cells are effectively enhanced.

Photovoltaic Characteristics of Nanowire CdS-CdTe-MoO_{3-x}-Au solar cells. The performance of the nanowire CdS-CdTe solar cells with MoO₃/Au back contacts was characterized. Figure 4 shows

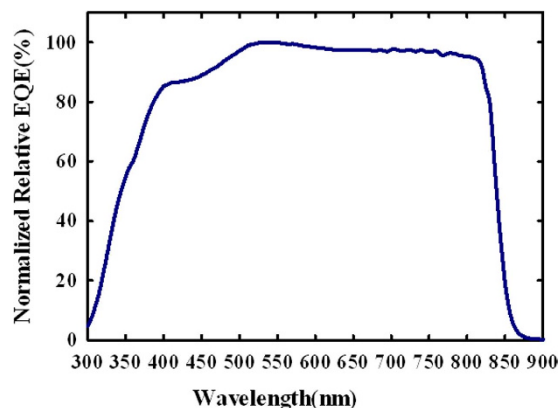


Figure 3. Normalized relative EQE of the nanowire CdS/CdTe solar cells on intrinsic SnO₂/ITO/Soda-lime glass substrate.

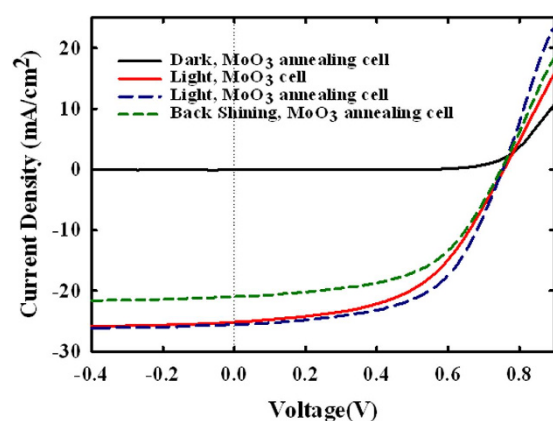


Figure 4. J-V curves of nanowire CdS-CdTe solar cells with as deposited MoO₃/Au back contacts under front side illumination, annealing MoO₃/Au back contacts under dark, front side and back side illuminations.

the J-V characteristics of the nanowire solar cells with MoO₃/Au contacts with N₂ annealing under dark, 1-Sun front side illumination and 1-Sun back side illumination, as well as the cells with MoO₃/Au contacts without N₂ annealing under 1-Sun front side illumination. There is no roll-over effect observed in any of the light J-V curves. Hence, incorporation of MoO₃/Au as a back contact to CdTe film eliminates the commonly observed blockage to hole transport across the interface between the CdTe layer and the “traditional” back contact. It has been reported that MoO₃ has high work function of 5.5 eV–6.86 eV and has a behavior like that of a metal^{15,16}. This high work function of MoO₃ is thought to form a well-aligned buffer layer and to reduce the effective barrier height, thus facilitating the formation of quasi-ohmic back contacts to CdTe.

The optimal thickness of the MoO₃ layer is observed to be in the 5 nm–10 nm range, while the thickness of CdTe by closed-space sublimation is about 10 μm–12 μm. Thinner MoO₃ layer, less than 5 nm, is not enough to guarantee a continuous coverage and efficient contacts for hole transport due to surface roughness of CdTe. Thicker MoO₃ layer, more than 10 nm, leads to decrease of short current density (J_{sc}) and fill factor (FF) due to high resistivity of the MoO₃ layer. To reduce resistance and guarantee a continuous layer, we deposited the 10 nm MoO₃ layer as the buffer layer of back contacts for CdTe absorber in this work. Table 1 summarizes cell performance parameters.

The 195 nm roughness value of the surface of the CdTe absorber layer is small enough that a conformal covering of the MoO_x electrode layer over CdTe is obtained when the thickness of MoO_x is more than 5 nm. When the thickness of the MoO_x buffer layer was smaller than 5 nm, the current-voltage characteristics of the completed NW-CdS/CdTe cell exhibited the “roll-over effect”, which is associated with a non-conducting, Schottky diode behavior at the CdTe-electrode interface. This would be expected to happen when the CdTe was not fully covered by the MoO_x buffer layer; then, there would be patches of CdTe surface in direct contact with the Au electrode, which forms a Schottky diode with p-CdTe. To avoid this undesirable outcome, in our experiments, the thickness of the MoO_x buffer layer was set at 10 nm.

Back Contacts	Illumination Conditions	J_{sc} (mA/cm ²)	V_{oc} (mV)	FF(%)	Efficiency (%)	R_s (Ω /cm ²)	R_{sh} (Ω /cm ²)
MoO ₃ /Au	Front-Side	24.8–25.4	755–756	52–52.2	9.77–10	9.8–10.13	300–308
MoO ₃ /Au annealing	Front-Side	25.4–25.8	752–753	56.9–57.2	10.9–11.12	7.58–7.78	328–336
MoO ₃ /Au annealing	Back-Side	20.7–21.4	749–750	55.1–55.2	8.55–8.84	9.93–10.35	338–350

Table 1. Photovoltaic properties of nanowire CdS-CdTe solar cells with MoO₃/Au as back contacts (Ranges of Variability).

Back Contacts	Illumination Conditions	J_{sc} (mA/cm ²)	V_{oc} (mV)	FF(%)	Efficiency (%)	R_s (Ω /cm ²)	R_{sh} (Ω /cm ²)
MoO ₃ /Au	Front-Side	25.1	755	52.1	9.97	9.97	303.6
MoO ₃ /Au annealing	Front-Side	25.6	752	57.1	11	7.69	332.2
MoO ₃ /Au annealing	Back-Side	21	749	55.1	8.67	10.1	344

Table 2. Photovoltaic properties of nanowire CdS-CdTe solar cells with MoO₃/Au back contacts (Average Values).

The reported cell performance was achieved on intrinsic SnO₂/ITO-soda-lime glass substrates and without antireflective coating.

The new Table 1 lists the variability range for each parameter for a statistical sample of 3; the average value for each parameter is listed in the new Table 2. Comparing the first two rows of the Efficiency column in these Tables, it is seen that the annealing step improved the average efficiency value by 1.03% (from 9.97% to 11%); this increase is much larger than the variability range values of 0.23% and 0.22% and, therefore, of practical significance.

Similarly, comparing the last two rows of the Efficiency column in these Tables, it is seen that under back side illumination, the average efficiency value decreased by 2.33% (from 11% to 8.67%); this reduction is much larger in magnitude than the variability range values of 0.29% and 0.22% and, therefore, of practical significance.

As comparison, these solar cell parameter values are lower than the V_{oc} of 770 mV, J_{sc} of 26 mA/cm², fill factor of 60% s, and power conversion efficiency of 12% seen in the best nanowire CdS-CdTe solar cell with Cu/graphite back contacts^{18,19}. Hence there is room for further optimization and performance improvement. Low shunt resistance might have been caused by contribution from the incomplete isolation of cells and less than satisfactory scribing of intrinsic SnO₂. Lower fill factor and J_{sc} are attributed to high series resistance, which is higher than the series resistance of planar CdS-CdTe solar cells. Fully stoichiometric MoO₃ with only Mo⁶⁺ is insulating and has a rather high resistivity of 10³–10⁴ Ω cm^{18,19}. Although J-V curves show that the incorporation of thin MoO₃ layer does not lead to the roll-over behavior, still, high resistivity attribute of MoO₃ may lead to some blockage of hole transport. This would show up as a high effective series resistance, leading to lower values fill factor and J_{sc} .

When MoO₃ is exposed to N₂ annealing before depositing Au as back contact, the performance of the nanowire solar cells is improved. The average J_{sc} and fill factor are improved to 25.6 mA/cm² and 57.1% respectively, and the average series resistance is reduced from 9.97 Ω /cm² to 7.69 Ω /cm², and shunt resistance is increased to 332.2 Ω /cm², leading to power conversion efficiency of approximately 11%. The measured error of the efficiency is 1%. It has been reported earlier that after annealing in N₂, a small amount of MoO₂ as well as Mo⁴⁺ ions are present in the MoO₃ film, and MoO₂ is metallic^{15,16}. Consequently, it is thought that after annealing at 200 °C in N₂ for 10 minutes, evaporated MoO₃ film has in it the mixed oxidation states of Mo, mainly attributed to MoO₃ and MoO₂ phases^{14–16}. These mixed oxidation states of Mo (MoO_{3-x}) can sustain the dominant high work function behavior arising from MoO₃ and also reduce resistivity due to metallic behavior of MoO₂ phase. Hence, series resistance of the nanowire solar cells is significantly reduced, and fill factor and power conversion efficiency are improved. An increase in J_{sc} for the annealing MoO₃ (MoO_{3-x}) back contact case is attributed to reduced barrier height due to lower resistivity of MoO_{3-x}/Au back contacts.

To illustrate the feasibility of a relatively transparent MoO_{3-x}/Au hole selective contact to p-CdTe, we illuminated the nanowire solar cells from back-contact side (MoO_{3-x}/Au side rather than SnO₂/ITO/Soda-lime glass side). The resulting J-V characteristics and the photovoltaic performance are shown in Fig. 4 and Table 1. Under back side illumination, the nanowire CdS-CdTe solar cell with MoO_{3-x}/Au back contact exhibits average J_{sc} of 21 mA/cm², V_{oc} of 749 mV, fill factor of 55.1%, corresponding to an average power conversion efficiency of 8.67%; this is much higher than the 5.8% value reported for the nanopillar CdS-CdTe solar cells with Cu/Au (1 nm/13 nm) back contacts from back side illumination²⁰.

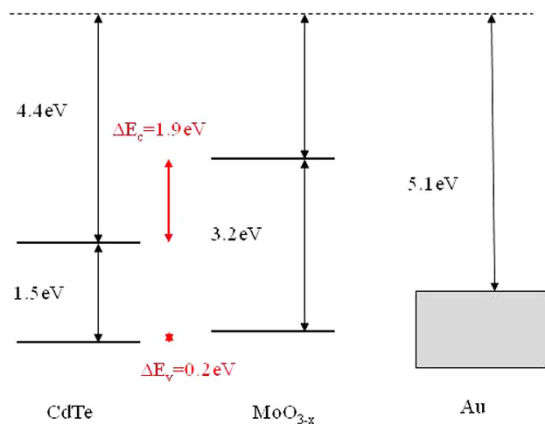


Figure 5. Energy Band Discontinuities between the CdTe absorber and the MoO_{3-x}/Au back contact layers.

When comparing with front-side illumination, thicker MoO_{3-x} (10 nm) and Au (15 nm) are responsible for low optical transmission. Although MoO_{3-x} has bandgap of 3.0–3.8 eV and high transparency of more than 80% from 400 nm to near IR range, still, Au of 15 nm thickness could cause relatively strong transmission losses. Hence, obvious decrease in efficiency is on account of lower J_{sc} based on low transmission from back side illumination. By further exploring transparent back contacts of CdTe, for example, transparent metal at nanoscale in the future, the superstrate structured nanowire CdS-CdTe solar cells on Al substrate can become a low complexity and high efficiency solar technique.

Considering that MoO_{3-x} behaves like a high work function metal with a low density of states at the Fermi level and has transparent properties in the visible and near IR range^{14,15}, it is chosen as a transparent back contact candidate for nanowire CdS-CdTe solar cells. For a better understanding of the MoO_{3-x}/Au back contacts, the energy band diagram of the junction between CdTe and MoO_{3-x}/Au is illustrated in Fig. 5 below. A work function of 5.7 eV and energy bandgap of 3.2 eV are assumed for MoO_{3-x} and the electron affinity of 4.4 eV and energy band of 1.5 eV are assumed for CdTe¹⁴. Figure 5 illustrates the energy band discontinuities between CdTe and MoO_{3-x}/Au. It is noted that Au, when placed directly next to p-CdTe, would form a blocking, Schottky diode contact with a barrier height of 0.8 eV. This would prevent hole transport from CdTe to Au contact and reduce cell performance. Introducing the thin MoO_{3-x} interlayer between CdTe and Au removes the Schottky diode problem. Now, a valence band offset of approximately 0.2 eV occurs between the CdTe and the MoO_{3-x} layers. Thus, MoO_{3-x} layer functions as a well-aligned buffer layer to reduce barrier height relative to CdTe. Hence it plays an important role to ensure hole extraction and transport to the electrode. As a result, the nanowire CdS-CdTe solar cells yield enhanced performance. In addition, due to its transparent properties, MoO_{3-x} layer, as a back contact to CdTe provides a potency to achieve superstrate structured nanowire solar cells on flexible metal foil substrate.

Our nanowire CdS-CdTe cell design with MoO_{3-x}/Au back contacts has demonstrated the performance comparable to that of planar counterpart with MoO_{3-x}/metal back contacts under front side illumination^{17–19}. For back side illumination, it has exhibited performance much better than that of nanopillar CdS-CdTe solar cells with Cu/Au contact²⁰, and its performance is comparable to that of planar CdS-CdTe solar cells with substrate structure^{7,21}. It clearly illustrates the concept of MoO_{3-x} as a transparent hole selective contact to p-CdTe due to its well-aligned band structure.

Conclusions and Future Work. We have fabricated nanowire CdS-CdTe solar cells and introduced MoO_{3-x} as a transparent, low barrier back contact. The MoO₃ layer reduces the valence band offset relative to the CdTe, and creates improved cell performance. Annealing as-deposited MoO₃ in N₂ reduces series resistance from 9.97 Ω/cm² to 7.69 Ω/cm², and hence efficiency of the nanowire solar cell is improved from 9.9% to 11%. When the nanowire solar cell is illuminated from MoO_{3-x}/Au side, it yields an efficiency of 8.67%. This reduction in efficiency is attributed to decrease in J_{sc} from 25.6 mA/cm² to 21 mA/cm² due to light transmission loss in the MoO_{3-x}/Au electrode. Even though these nanowire solar cells, when illuminated from back side exhibit better performance than that of nanopillar CdS-CdTe solar cells structure^{7,21}, further development of transparent back contacts of CdTe could enable a low-cost roll-to-roll fabrication process for the superstrate structure-nanowire solar cells on Al foil substrate.

Various potential improvements of our nanowire solar cell design with MoO_{3-x}/metal back contacts can be envisioned including optimization of MoO_{3-x} layer to further reduce resistance, and optimization of CdS nanowires and CdTe layer to further improve V_{oc} and J_{sc} . The FF could be improved by replacement or ideal scribing of intrinsic SnO₂ to increase shunt resistance and optimization of MoO_{3-x} layer for low series resistance. Development of a transparent metal layer on the MoO_{3-x} will improve light transmission loss and significantly enhance J_{sc} under back-side illumination. Furthermore, MoO_{3-x} with

the transparent metal as the back contacts of CdTe could make the nanowire solar cells on Al foil with superstrate structure promising and facilitate a roll-to-roll fabrication process application on such solar cells, thus providing a route toward a scalable, low-cost solar cell architecture.

References

1. Wu, X. High-efficiency polycrystalline CdTe thin-film solar cells. *Solar energy* **77**, 803–814 (2004).
2. Jackson, P. *et al.* New world record efficiency for Cu (In, Ga) Se₂ thin-film solar cells beyond 20%. *Progress in Photovoltaics: Research and Applications* **19**, 894–897 (2011).
3. Wang, W. *et al.* Device Characteristics of CZTSSe Thin-Film Solar Cells with 12.6% Efficiency. *Advanced Energy Materials* **4**, n/a-n/a doi: 10.1002/aenm.201301465 (2014).
4. Green, M. A., Emery, K., Hishikawa, Y., Warta, W. & Dunlop, E. D. Solar cell efficiency tables (version 39). *Progress in photovoltaics: research and applications* **20**, 12–20 (2012).
5. Liu, M., Johnston, M. B. & Snaith, H. J. Efficient planar heterojunction perovskite solar cells by vapour deposition. *Nature* **501**, 395–398 (2013).
6. Kranz, L. *et al.* Doping of polycrystalline CdTe for high-efficiency solar cells on flexible metal foil. *Nature communications* **4** (2013).
7. Aliyu, M. *et al.* Recent developments of flexible CdTe solar cells on metallic substrates: issues and prospects. *International Journal of Photoenergy* **2012**, doi: 10.1155/2012/351381 (2012).
8. Chen, D., Zhao, W. & Russell, T. P. P3HT nanopillars for organic photovoltaic devices nanoimprinted by AAO templates. *ACS nano* **6**, 1479–1485 (2012).
9. Tepavcevic, S., Darling, S. B., Dimitrijevic, N. M., Rajh, T. & Sibener, S. J. Improved hybrid solar cells via *in situ* UV polymerization. *Small* **5**, 1776–1783 (2009).
10. Ramanathan, M., S Michael Kilbey, I., Ji, Q., Hill, J. P. & Ariga, K. Materials self-assembly and fabrication in confined spaces. *Journal of Materials Chemistry* **22**, 10389–10405 (2012).
11. Ramanathan, M., Tseng, Y.-C., Ariga, K. & Darling, S. B. Emerging trends in metal-containing block copolymers: synthesis, self-assembly, and nanomanufacturing applications. *Journal of Materials Chemistry C* **1**, 2080–2091 (2013).
12. Dang, H., Rajaputra, S., Guduru, S. & Singh, V. Cadmium Sulfide Nanowire Arrays for Window Layer Applications in Solar Cells. *Solar Energy Materials and Solar Cells* **126**, 184–191 (2014).
13. Alonzo, J. *et al.* Assembly and organization of poly (3-hexylthiophene) brushes and their potential use as novel anode buffer layers for organic photovoltaics. *Nanoscale* **5**, 9357–9364 (2013).
14. Simchi, H., McCandless, B. E., Meng, T. & Shafarman, W. N. Structure and interface chemistry of MoO₃ back contacts in Cu (In, Ga) Se₂ thin film solar cells. *Journal of Applied Physics* **115**, 033514 (2014).
15. Battaglia, C. *et al.* Silicon heterojunction solar cell with passivated hole selective MoO_x contact. *Applied Physics Letters* **104**, 113902 (2014).
16. Battaglia, C. *et al.* Hole Selective MoO_x Contact for Silicon Solar Cells. *Nano letters* **14**, 967–971 (2014).
17. Lin, H., Xia, W., Wu, H. N. & Tang, C. CdS/CdTe solar cells with MoO_x as back contact buffers. *Applied Physics Letters* **97**, 123504–123504-123503 (2010).
18. Paudel, N. R., Compaan, A. D. & Yan, Y. Ultrathin CdTe Solar Cells with MoO_{3-x}/Au Back Contacts. *Journal of Electronic Materials* **43**, 2783–2787 (2014).
19. Paudel, N., Compaan, A. & Yan, Y. Sputtered CdS/CdTe solar cells with MoO_{3-x}/Au back contacts. *Solar Energy Materials and Solar Cells* **113**, 26–30 (2013).
20. Fan, Z. *et al.* Three-dimensional nanopillar-array photovoltaics on low-cost and flexible substrates. *Nature materials* **8**, 648–653 (2009).
21. Romeo, A. *et al.* Development of thin-film Cu (In, Ga) Se₂ and CdTe solar cells. *Progress in Photovoltaics: Research and Applications* **12**, 93–111 (2004).

Acknowledgements

This work was supported in part by grants from the National Science Foundation, (NSF-NIRT-ECS-0609064) and (NSF-EPCOR EPS-0447479), Department of Energy/Kentucky Renewable Energy Consortium (DE-FG36-05G085013/ULRF 05-1231G, (NSF-EPS-0447479) and by grants from the Kentucky Science and Engineering Foundation, (KSEF-148-502-02-27, KSEF- 148-502-03-68). The authors would like to thank PV measurements, Inc for quantum efficiency measurement, Dr. Suresh Rajaputra for SEM images and fabrication processes.

Author Contributions

H.D. designed and conducted the experiments, fabricated the solar cells, performed characterizations and analyzed data. V.S. conceived the idea and the overall project of the embedded nanowire layers in solar cells with MoO_x contacts, and analyzed the results of experimental measurements. H.D. and V.S. co-wrote the paper. All authors reviewed the manuscript.

Additional Information

Competing financial interests: The authors declare no competing financial interests.

How to cite this article: Dang, H. and Singh, V. P. Nanowire CdS-CdTe Solar Cells with Molybdenum Oxide as Contact. *Sci. Rep.* **5**, 14859; doi: 10.1038/srep14859 (2015).



This work is licensed under a Creative Commons Attribution 4.0 International License. The images or other third party material in this article are included in the article's Creative Commons license, unless indicated otherwise in the credit line; if the material is not included under the Creative Commons license, users will need to obtain permission from the license holder to reproduce the material. To view a copy of this license, visit <http://creativecommons.org/licenses/by/4.0/>